Damage Assessment in AISI/SAE 8620 Steel and in a Sintered Fe-P Alloy by Using Acoustic Emission

E.S. Palma and T.R. Mansur

(Submitted 4 October 2002; in revised form 11 October 2002)

Mechanical behavior of an AISI/SAE 8620 steel and of a sintered Fe-P alloy has been investigated using acoustic emission signals. Four-point bending tests were carried out using strain gages to measure the deformation. The onset of plastic strain was determined through the acoustic signal. The acoustic signal of the sintered material was very strong and increased continually with external load. The correlation between microstructure and signal acoustic is discussed.

Keywords acoustic emission, damage, mechanical behavior, porosity, sintered materials

1. Introduction

In a limited sense, damage in metals is the process of nucleation and growth of micro-cracks and cavities. For engineers, damage of materials is the progressive physical process by which materials break. At the microscale level, this is the accumulation of microstresses in the vicinity of defects and interfaces, which results in breaking of the atomic bonds. At the macroscale level, the coalescence of microcracks or microvoids nucleates a crack, which tends to grow under the influence of stress. In a wider sense, damage is any process that impedes or limits a machine from operating as expected.

According to Fig. 1, the damage D in a body with defects can be determined using Eq 1,

$$D = \frac{S_T - S_O}{S_T} = \frac{S_D}{S_T} \quad \text{(Eq 1)}$$

where S_T is the total section area, defined by the normal n, and S_O is the effective resisting area (Fig. 1). $D = 0$ corresponds to the undamaged state. The fracture of material occurs when damage (D) becomes large enough, and reaches a critical value D_C, that is $D = D_C$.[1]

Damage can manifest in several ways depending upon (a) the nature of materials, (b) the type of loading, and (c) environment conditions. Brittle fracture, ductile fracture, creep, and fatigue are important manifestations of damage in engineering practice.

There are several ways to measure damage in a component. One of the simplest ways is direct measurement through evaluating total cracked areas lying on a surface. These areas are determined using quantitative image analysis. Thus, damage

E.S. Palma, Department of Mechanical Engineering, Pontifical Catholic University of Minas Gerais—PUC Minas, Belo Horizonte, Brazil; and **T.R. Mansur,** Nuclear Technology Research Center—CDTN/CNEN, Belo Horizonte, Brazil. Contact e-mail: palma@pucminas.br.

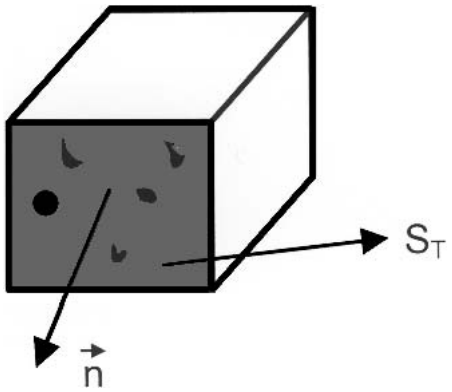

Fig. 1 Definition of damage

can be obtained by dividing the area of microcracks or microcavities (S_D) by the total area S_T:

$$D = \frac{S_D}{S_T} \quad \text{(Eq 2)}$$

Variation of elasticity modulus is a non-direct measurement based on an influence of damage on elasticity. It is determined using the relationship

$$D = 1 - \frac{E_{ef}}{E} \quad \text{(Eq 3)}$$

E and E_{ef} are the undamaged and damaged elastic modulus, respectively.

1.1 Acoustic Emission

Acoustic emission (AE) is the elastic energy that is spontaneously released by materials when they are subjected to loading. Acoustic emission testing is a passive, receptive technique analyzing ultra sound pulses emitted by a defect at in the moment of its occurrence. The capacity of detecting weak signals makes acoustic emission an important technique for monitoring damage. The AE is nondestructive and has long been used in structural engineering to characterize crack nucleation and growth.[2-4] Onset of plastic deformation can also been determined using this technique.[5,6] The methodology for lo-

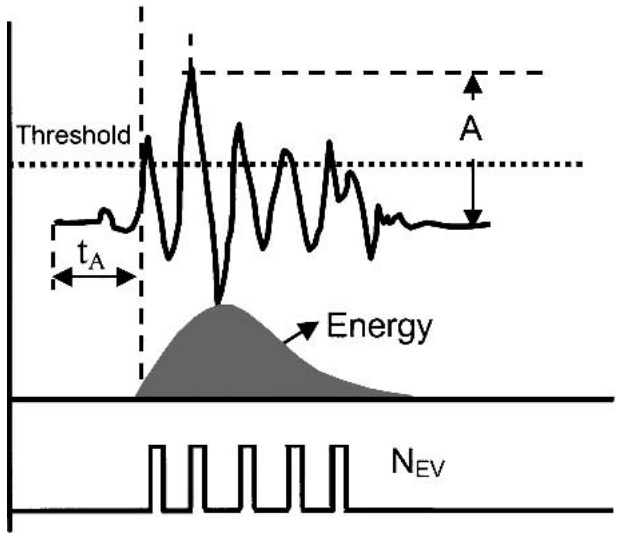

Fig. 2 Some parameters of acoustic emission

cating the AE source and for calculating wave velocity in a damaged material has also been well developed.[2,7]

The AE response is influenced by material properties and testing conditions. Among others factors, high strength and strain rates, non homogeneity, materials containing discontinuities, and crack propagation, all tend to increase AE response.[8,9]

There are two types of AE signals: transient and continuous signals. The beginning and end of the transient signal (also called burst) deviates clearly from background noise. AE signal is characterized by the following parameters:[2] peak amplitude (A), energy E (integral of the squared amplitude over time of signal duration), number of threshold crossings (counts or N_{EV}), and arrival time (t_a) (Fig. 2).

Thus, careful measurements of emission activity as a function of time or stress are used to give insight into the dynamics of mechanical behavior of materials. Although AE has long been used, there is limited research using this technique for sintered alloys. The goal of this study is to compare the mechanical behavior of a sintered Fe-P alloy with a commercial pore-free AISI 8620 steel. Emphasis is given to the correlation between acoustic signal and microstructure of the materials.

2. Experimental Procedure

2.1 Materials The raw materials used in this investigation were an AISI 8620 steel and a sintered Fe-P alloy having a residual porosity of $P_O = 6.5\%$. The chemical composition of the two materials is given in Table 1.

This sintered material was made from a mixture of elemental iron powder and pre-alloyed iron-phosphorus powder with 0.5 wt.% lubricant (zinc stearate). Four-point bend specimens were produced using a floating die tool. The applied pressure was such that a residual porosity $P_O = 6.5\%$ was produced. Sintering of the specimen was carried out for 40 min. at 1150 °C in an 80% nitrogen-20% hydrogen atmosphere. Final dimensions of the specimen (Fig. 3) for both materials were achieved by machining.

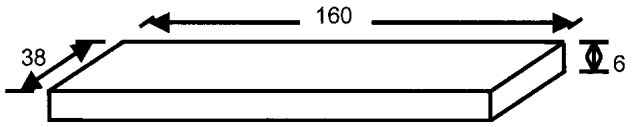

Fig. 3 Bending specimens, mm

Table 1 Chemical Composition for the Materials Used

Element wt.%	C	Si	Mn	Cr	Ni	Mo	P
AISI 8620	0.20	0.18	0.80	0.50	0.55	0.20	<0.03
Fe-P	0.03	0.13	0.12	0.07	0.06	···	0.45

2.2 Methodology The four-point bend tests were carried out on a 100 kN, Universal Testing Machine (UTM) at a crosshead speed of 0.18 mm/min (Fig. 4). Strain gauges (Model TA-06-455JB-350—Micro Measurements Group, Vishay Measurements Group, Inc., Raleigh, NC), having a gauge factor $F = 2.05$ and resistance $R = 350.0 \pm 0.5\%$, were mounted in some specimens. The specimens were loaded and deformation was measured using the strain gauge mounted on the tensile face. To minimize friction, the points of application of force and bearing were lubricated. Some specimens were loaded, unloaded, and loaded again. The cycle was repeated 3-4 times for each specimen. Stresses were calculated using the equation

$$\sigma = \frac{M}{W} = \frac{6M}{bh^2} = \frac{3FL}{bh^2} \quad \text{(Eq 4)}$$

where M is the external bending moment, W is the section modulus, L is the length, b the width, and h is the thickness of the specimen. For dimensions of the used specimens, the stress is a function of the applied force (F):

$$\sigma = 65\,789 \times 10^{-3}\,F \quad \text{(Eq 5)}$$

Acoustic emission signals were measured using an apparatus consisting of transducers, preamplifiers, and a signal acquisition and treatment system. For a transducer, two Model R15I acoustic resonant sensors were used (Physical Acoustic Corporation—PAC, Princeton, NJ). The properties of these sensors are summarized in Table 2. The acoustic sensors were magnetically attached to the tensile side of each specimen (Fig. 4). To ensure continuous transmission of acoustic emission waves from the structure to the sensors, grease was used as a coupling medium. The efficiency of mounting and coupling was done by breaking the lead of a pencil and determining the distance of the source from the center of the sensor.

The sampling frequency for all tests was 4 MHz. The output signal from the AE sensor was passed through an integral preamplifier (x100 gain), which is mounted onto the same housing. The signal acquisition and treatment system with four available channels (Model PCI-DSP4 [PAC]) is constituted by a PCI card that is inserted in a computer. The system has transfer capacity of up to 132 MB/s. The frequency measuring range is set by the operator. There are four low pass and four high pass filters available for each channel. A band pass filter was used with a passband of 100-200 kHz. To connect the

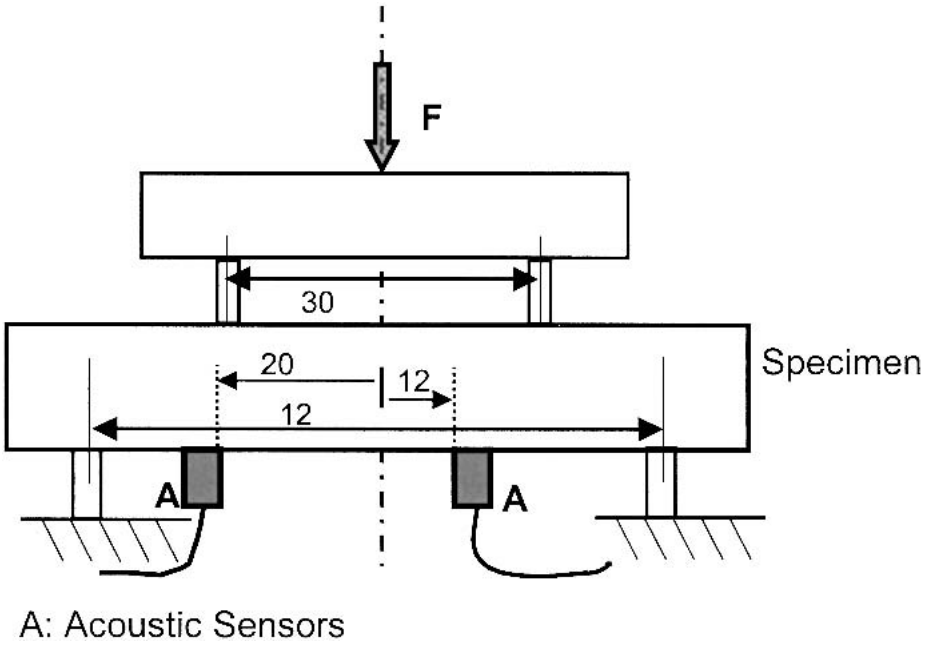

Fig. 4 Four-point bend test configuration

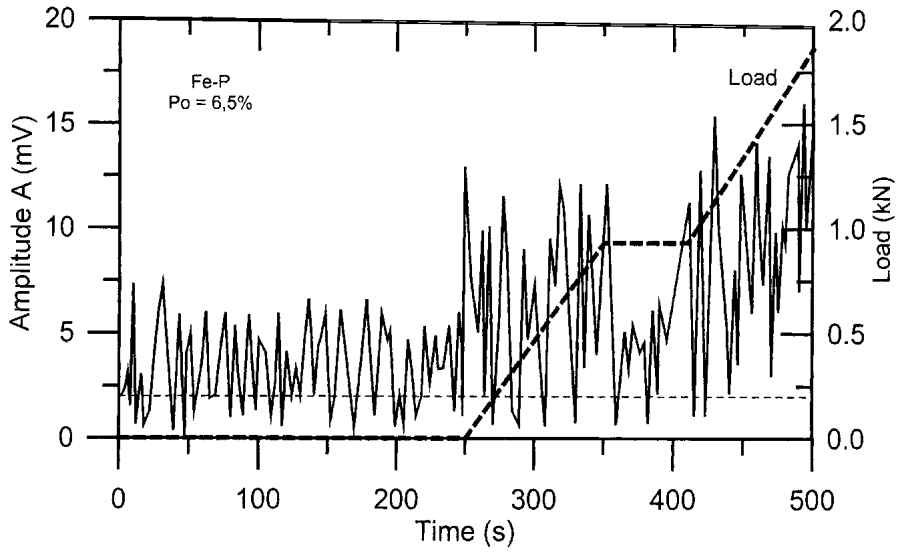

Fig. 5 Preliminary test for noise detection-sintered Fe-P

Table 2 Acoustic Sensor Properties (PAC)

Dimensions: Diameter × Height, mm	Operation Frequency, kHz	Resonant Frequency, kHz
29 × 31	70-200	153

preamplifier to the computer, coaxial cables RG-58/AU, having a resistance of R = 50Ω, were used.

To measure acoustic signal, the parameters shown in Fig. 2 were used: peak amplitude (A), energy E (integral of the squared amplitude over time of signal duration), number of threshold crossings (Counts or N_{EV}), and arrival time (t_a).

Table 3 Mechanical Properties of the Materials Used

Material	Yield Stress $\sigma_{0.2}$ MPa	UTS, σ_R MPa	Elasticity Modulus, MPa
SAE 8620	370 ± 10	602 ± 24	209 000
Fe-P	143 ± 9	278 ± 11	189 000

3. Experimental Results and Discussion

The mechanical properties of used materials are given in Table 3. The properties were obtained from an average of three tests on each material. An event may be simulated on the

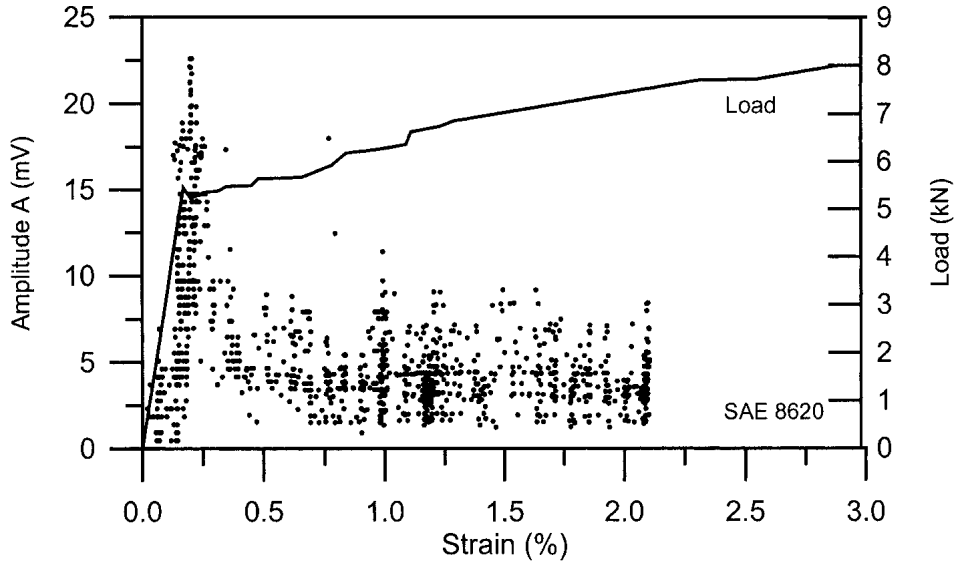

Fig. 6 Correlation between acoustic emission (amplitude) and deformation-SAE 8620

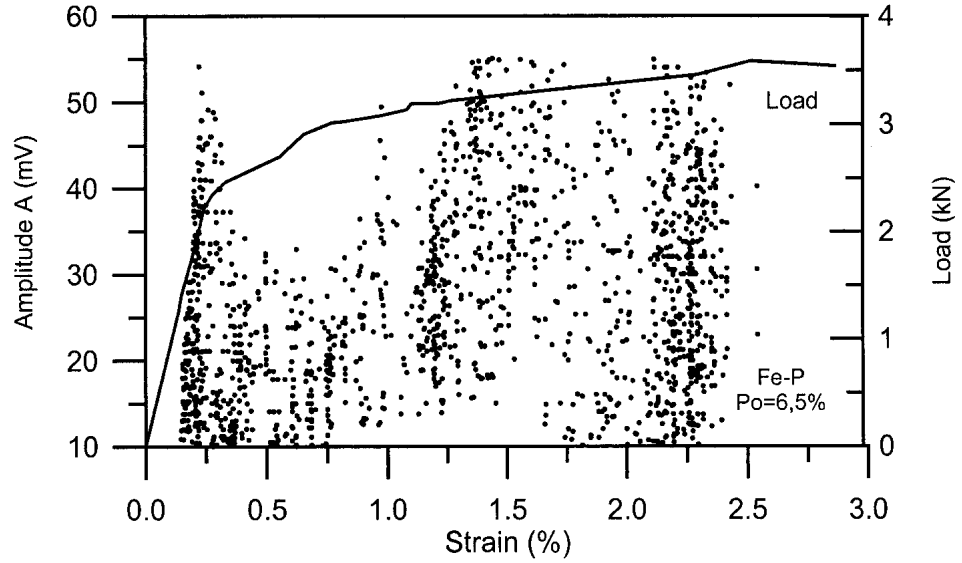

Fig. 7 Correlation between acoustic emission (amplitude) and deformation-sintered material

specimen surface to check system/channel performance or to determine sensor spacing. Thus, a lead was broken at the middle of the specimen surface, 12 and 20 mm away from the sensors 1 and 2, respectively. The breaking of lead creates a reproducible stress wave packet traveling through the metal, which is sensed by the AE sensor. The source distances from sensors 1 and 2, determined by the AE system were 10.9 ± 0.6 and 21.6 ± 0.8 mm, respectively. Thus, an error between the experimental and actual values was approximately 10%.

Besides, preliminary tests were performed to check for complete installation and concurrently determine the threshold level. The system works with no applied load during 250 s. After this time, the load was applied up to approximately 1 kN for sintered materials and up to 1.7 kN for SAE 8620 steel (well below the yield stress for both materials). The loads were held constant for 50s and increased again up to 1.7 and 3.8 kN for sintered material and SAE 8620 steel, respectively. While no loads were applied, it was observed signals with amplitude values up to 8 mV. At the instant of applying force on SAE 8620 specimens was observed amplitudes of approximately 12 mV, decreasing again to 8 mV. After applying load to the sintered material, the amplitude did not return to previous values, maintained at around 15 mV, as shown in Fig. 5. Thus, after these tests, the threshold value was set to 10 mV. This threshold value together with filter selection was able to minimize the influence of noise. Higher frequencies attenuate faster; hence they have a smaller detection distance. Background noise coming from longer distances consists of fre-

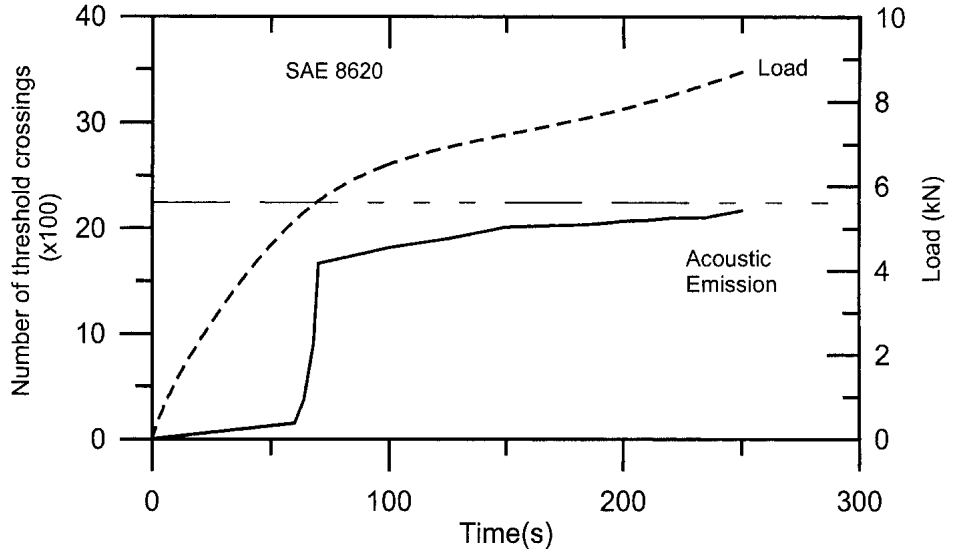

Fig. 8 Number of threshold crossings (counts or N_{EV}), SAE steel

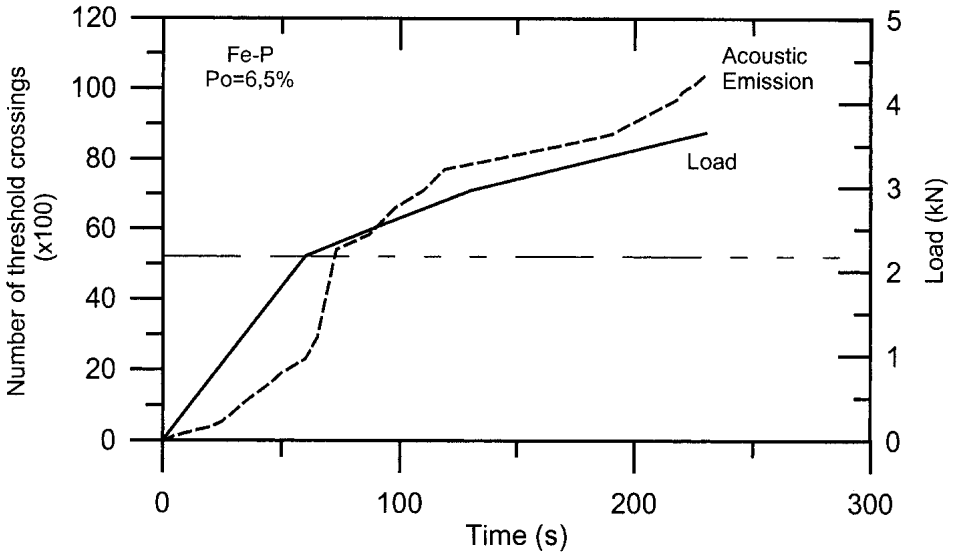

Fig. 9 Number of threshold crossings (counts or N_{EV}), sintered material

quency components below 100 kHz,[10] so they have minimal influence on measurement chain tuned to 100-200 kHz.

The correlation between acoustic emission and strain for the SAE 8620 steel subjected to axial external load are shown in Fig. 6. Amplitude increases rapidly with the onset of yield. Before and after the yield strain, the acoustic emission in this material is small, with amplitude values up to 10 mV.

The acoustic emission was intense during tests on sintered materials (Fig. 7). The amplitude values are larger than those observed in the pore-free steel. It was also observed that amplitude peaks at the onset of yield strain.

However, in contrast to the SAE 8620 steel, following the yield strain, the acoustic activity increases with increasing load. A deeper analysis of the acoustic emission signals from both materials is done by comparing Fig. 8 with Fig. 9. The number of threshold crossings (Counts or N_{EV}) increases continually with increasing load for the sintered material. For the SAE 8620 tests, after an increase at the onset of yield strain, the number of threshold crossings remains constant. Residual porosity in the microstructure of sintered materials is the reason for this difference. It is known that pores have a decisive influence on mechanical behavior of these materials.[11-13] It was observed that for even light loads crack initiation and crack propagation takes place. In addition to cracks that propagate quickly to a certain length and stop growing but open up further with increasing load, the pores become larger and weaken the cross section. Thus, cracks and heterogeneous plastic strain cause high acoustic emission activity in these materials.

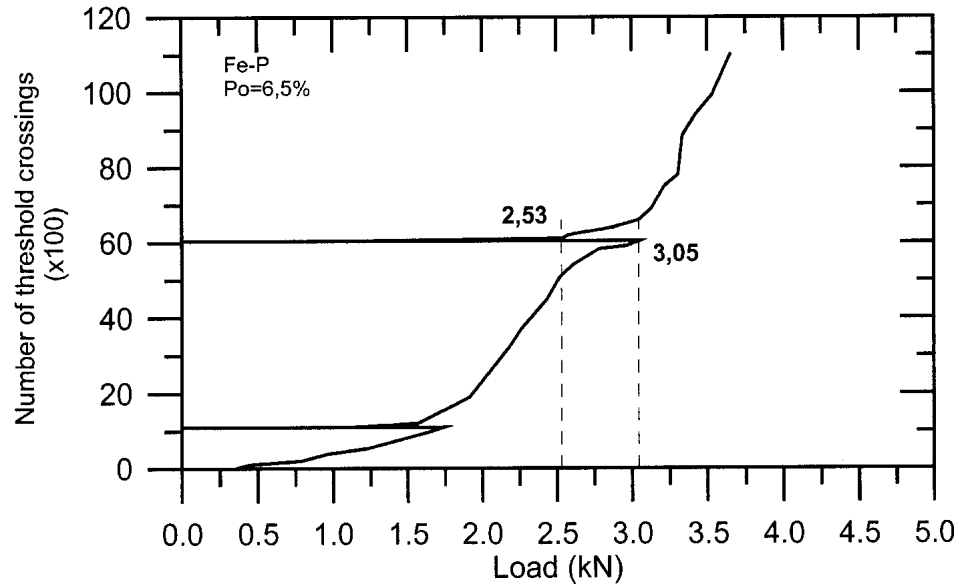

Fig. 10 Felicity ratio determination in sintered materials

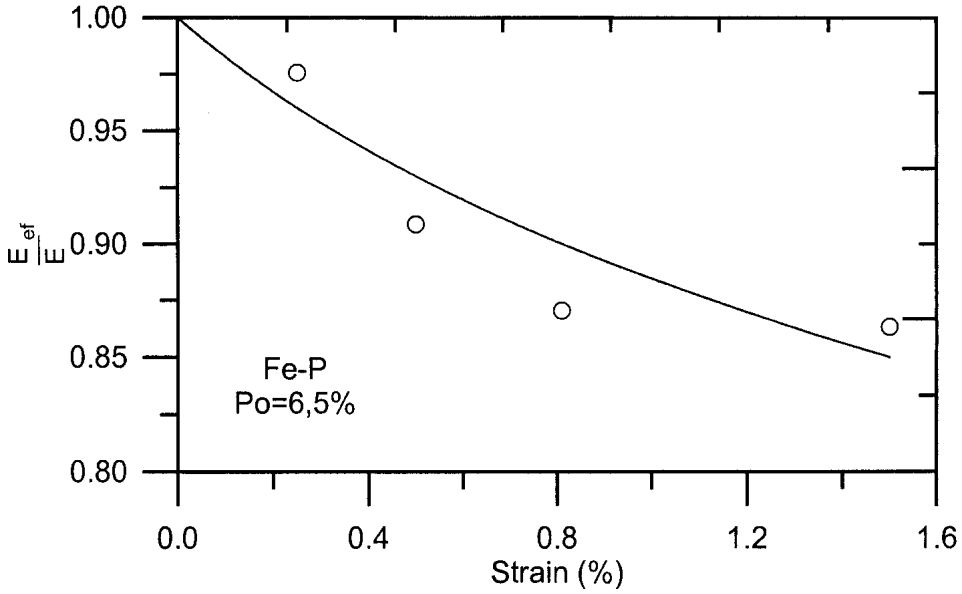

Fig. 11 Porosity influence on the elastic modulus of sintered materials

The correlation between mechanical behavior and acoustic emission is better understood by determining the felicity ratio and Kaiser effect of the materials. Kaiser effect is known as an irreversible AE generating behavior under stress. It results because cracks nucleated during prior loading do not propagate until the load exceeds the former level in subsequent loading.[2,3] Thus, for materials that obey the Kaiser effect, no emission will be observed during a load cycle until the previous maximum load is reached. Acoustic emissions between loads, before the previous maximum is reached, mean that the Kaiser effect is not obeyed and the felicity ratio (*FR*) can be determined. This effect in sintered materials is shown in Fig. 10. Emission is observed upon initial loading up to approximately 1.8 kN, but not upon unloading. Upon reapplying the load, there is no emission (line is horizontal) until approximately 1.5 kN. At this time, the acoustic emission begins (i.e., before reaching the previous maximum load of 1.8 kN). To quantify this phenomenon, *FR* is determined by dividing the load at which emission begins (P_{BEG}) by the previous maximum load (P_{MAX}),

$$FR = \frac{P_{BEG}}{P_{MAX}} \quad \text{(Eq 6)}$$

During the first cycle, the FR of sintered material was 0.90. The load is increased up to 3.05 kN, with more emission, and another unload-reload cycle is applied. This time, due to higher stress levels coupled with the influence of porosity, significant defects begin to emit at load equal to 2.53 kN. The FR ratio in this cycle was 0.83 (i.e., 10% smaller than the previous value). These tests were performed for the pore-free SAE 8620 steel and FR was equal to unity (i.e., this material obeyed the Kaiser effect).

A narrow correlation exists between acoustic emission and mechanical behavior of sintered materials. During the load-unload-reload tests the elastic modulus was determined from slope of the corresponding stress-strain graph, and the results are shown in Fig. 11. A strong influence of porosity leads to a decrease in elastic modulus, as the load (and strain) increases. This is caused by porosity (as explained previously) and is in accordance with calculated values of FR.

4. Conclusions

This study attempted to devise a simple and cost-effective, reliable method of measuring damage in engineering materials. In summary, the results presented serve three purposes:

- They demonstrate that acoustic emission is well suitable for damage detection of steel specimens submitted to load in labor conditions.
- They allow failure correlations with microstructure of the sintered materials during the test.
- More generally, they show the very good potential of an effective use of in-situ AE for monitoring experiments of heterogeneous materials.

Acknowledgments

This research was performed with the financial support of the Fundação de Amparo à Pesquisa de Minas Gerais (FAPEMIG) with additional assistance from the CNPq (Brasilian National Research Bureau).

References

1. J. Lemaitre: *A Course on Damage Mechanics,* Springer Verlag, Berlin, Germany, 1996.
2. A.A. Pollock: "Acoustic Emission Inspection" in *Metals Handbook,* Vol. 17, 9th ed., ASM International, Materials Park, OH, 1989, pp. 278-94.
3. C.B. Scruby: "Quantitative Acoustic Emission Techniques" in *Research. Techniques in Nondestructive Tests*, Vol. III, Academic Press, NY, 1985, pp. 141-210.
4. P. Rizzo and F. Lanza di Scalea: "Acoustic Emission Monitoring of Carbon-Fiber-Reinforcing-Polymer Bridge Stay Cables in Large Scale Testing, Experimental Mechanics," 2001, *4*(3), pp. 282-90.
5. M.A. Hamstad and J.D. McColskey: "Detectability of Slow Crack Growth in Bridge Steels by Acoustic Emission," *Mater. Eval.*, 1999, *57*(11), pp. 1165-74.
6. M.A. Hamstad: "Acoustic Emission on 304 Stainless Steel," *Metal Sci.*, 1981, *15,* pp. 541-48.
7. Z.J. Li and S. P. Shah: "Localization on Microcracking in Concrete Under Uniaxial Tension," *ACI Mater. J.*, 1994, *91*, pp. 372-81.
8. R.K. Miller and P. McIntire: "Acoustic Emission Testing" in *Nondestructive Testing Handbook*, Vol. 5, 2nd ed., American Society for Nondestructive Testing, Columbus, OH, 1985.
9. T.F. Drouillard and T.G. Glenn: "Production Acoustic Emission Testing of Braze Joint," *J. Acoust. Emiss.*, 1985, *1*(2), pp. 81-85.
10. S.O. Fahey and A.L. Wicks: "Noise Sources in Mechanical Measurements," *Exp. Tech.*, 2000, March/April, pp. 40-43.
11. H.E. Exner and D. Pohl: "Fracture Behavior of Sintered Iron," *Powder Metall. Int.*, 1978, *10*(4), pp. 193-96.
12. J.R. Moon: "Elastic Moduli of Powder Metallurgy Steels," *Powder Metall.*, 1989, *32*(2), pp. 132-39.
13. T.J. Griffiths and A. Ghanizadeh: "Determination of Elastic Constants for Porous Sintered Iron Powder Compacts," *Powder Metall.*, 1986, *29*(2), pp. 129-33.